Stereoscopic image sensor with low-cost RGB filters tunned for the visible range

J. P. Carmo, R. P. Rocha, M. F. Silva, D. S. Ferreira, J. F. Ribeiro, and J. H. Correia
Dept. Industrial Electronics, University of Minho, Campus Azurem, 4800-058 Guimaraes, Portugal
Email: jcarmo@dei.uminho.pt, phone/fax: +351-253510-190/+351-253510-189

Abstract - **This paper presents a low-cost technology for fabricating optical filters arrays tuned for the primary colors. The fabrication process presented in this paper is intended for directly printing the optical filters into a transparent flexible substrate (acetate). The target application of these optical filters is for enabling the acquisition of multicolor stereoscopic images with a sensor made in CMOS technology.**

Keywords – Low-cost production, optical filters, RGB, image sensor, stereoscopic vision,CMOS.

I. INTRODUCTION

The available image sensors are not ready for stereoscopic acquisition. The stereoscopic vision as well as the high resolution enhances the quality of the images. The traditional solutions for acquiring tridimensional images are based on two or three monoscopic cameras, which must be perfectly synchronized with the penalty of losing the tridimensional effect or the emergence of artifacts in the images [1]. Moreover, it is very common the use of both depth sensors and monoscopic image sensors for doing the conversion between the bidimensional to the tridimensional domain [1]. The stereoscopic vision uses the parallax effect to *cheat* the brain for making it gain depth perception (which is also known as stereopsis), and thus the name "stereoscopy". This means that a stereoscopy with bad quality consequently induces perceptual ambiguity into the viewer [2]. This happens because the human brain is much more sensitive and less tolerant to bad stereoscopic images than to monocular images. Thus, a conscious of double vision can be caused by a multiplicity of factors, but all due to differences between the right and left images. The nature of such differences can be due to differences in brightness, differences in contrast, changes in reflection angle, differences in colors, and so on. Additionally, and according to the media experts, (even better) tridimensional image sequences can take few milliseconds to allow the brain and eyes to naturally adapt, to get the scene and adjust to it.

An emergent application field for this kind of image sensors is in wireless endoscopic capsules, where the pictures are acquired during its course through the digestive tract after being swallowed [3][4], opening new solutions in non-invasive examination methods. Also, high-resolution/high-quality images allow a further step behind the next generation of the camera in a pill, which has the same size as a normal camera pill. In a near future, it is expected that the continuous developments observed in the Microsystems field can be used to extend the functions behind simple image acquisitions, which means that once swallowed and passing naturally through the digestive track, the camera pill can be electronically programmed to control the delivery of medicine according to a pre-defined drug release profile. The pill determines its location in the intestinal tract by measuring the local acidity of its environment. Distinct areas of the intestinal tract have distinct pH profiles, thus the location can be determined with good accuracy. The pill releases medicine from its drug reservoir via a microprocessor controlled pump, allowing accurate programmable drug delivery. In addition, as in the case of stereoscopic image acquisitions, the capsule can be designed to measure local temperature, and report measurements wirelessly to an external receiver unit. Furthermore, this innovative image sensor will enjoy all CMOS imaging advantages. The use of CMOS technology will have the advantage to decrease the total power consumption of the sensor, and unlike conventional CCD technology, CMOS sensors use the same manufacturing platform as most microprocessors and memory chips. Therefore, the CMOS devices are more cost-effective and easier to produce in comparison to CCDs. An appropriate low-power consumption CMOS process opens the doors for using thin-films integrated batteries with silicon compatibility [5] and low-toxicity [6]. The exceptional characteristics of the proposed image sensor make it suitable for endoscopic capsules integration with thin-film batteries as power sources. The 0.7 μm CMOS process from the AMIS foundry is the one that allows the fabrication of the photodetectors and read-out electronics with the smaller cost. Moreover, since this process is well characterized, the fast execution of prototypes is enabled.

II. IMAGE SENSOR ARCHITECTURE

The stereoscopic image sensor concept presented in this paper is composed by two entrance apertures (as it happens inside the human eyes) from where the left and right channels (the two images to be converted to the tridimensional domain) are passing before being focused by an objective lens into the sensitive area of the CMOS microdevice. The objective focus the two incident beams (two viewpoints) in the direction of the microlens, where the light is concentrated in a small area (i.e., into the sensitive area of the CMOS microdevice, where are located the photodiodes). After the passage by the optical filters, the individual rays of each left and right are directed towards the respective CMOS photodiodes. These two viewpoints are separated by focussing each side on the appropriate sensor column under the microlens and optical filters.

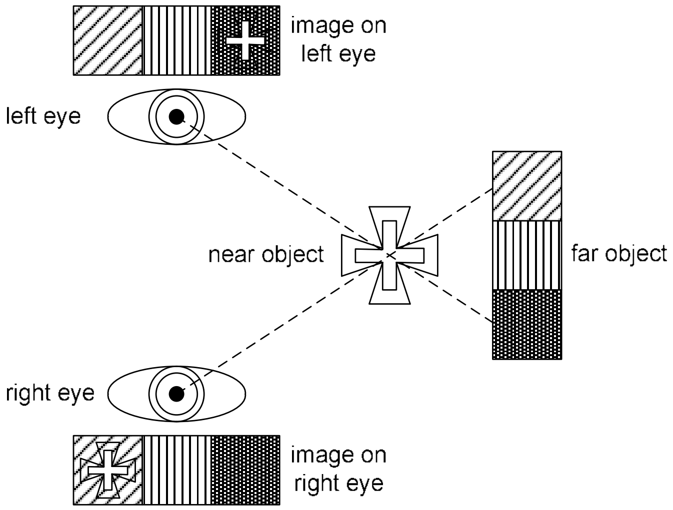

Figure 1: A schematic to illustrate the parallax effect for inducing sensation of deep into the human brain [1].

III. SENSOR FABRICATION

A. The structures of the stereoscopic image sensor

The photodetector is a n+/p-epilayer junction photodiode fabricated in a CMOS process, because it provides the best possible quantum efficiency in the desired spectral range of photodiodes available in a CMOS process. Moreover it yields the highest possible fill-factor, since a deep n-well is not required for every pixels [7]. In the 0.7 µm selected CMOS process, the junction depth of the photodiodes is fully defined and cannot be altered. However, the quantum efficiency can be improved by a suitable arrangement of dielectric layers on top of the photodiode surface. These act as a thin-film interference filter and influence the optical transmittance for each wavelength independent of the CMOS process. In this CMOS process there are three major dielectric layers above the photodiode p-n junction. The first oxide (boron phosphor silicate glass is the metal1-poly oxide) is above the photodiode. The second major oxide comprises those between the first and second metal layers. The last layer (overlayer) is made of silicon nitride. In the literature it can be found that a photodiode structure without two of the three dielectric layers above the pn-junction will provide the best quantum efficiency in the desired spectral range in a CMOS process [8]. Further improvements of fill-factor are expected by using the octogonal shape in the 4-neigbors pixels, because it provides a shared chip-area to integrate the next-to-the-pixel circuitry [9].

B. Optical filter fabrication

The thin-film deposition of a material in a carrier substrate (glass or quartz) is the common method to fabricate optical filters. Normally, the fabrication of thin-films with a band-pass around a given wavelength is done by successively depositing different dielectric materials in order to obtain a dielectric multilayer structure able to achieve that characteristic. For each primary color, the thin-films are designed to yield a given passband around the respective wavelengths. However, the fabrication of optical filters based on thin-films made of dielectric materials is complicated (in spite of well tuned and characterized) with a high number of process steps and thus, increased fabrication costs. The method proposed in this paper for fabricating optical filters can be implemented with low-cost because a standard color printer (with the suitable resolution ofcourse) and a sheet of acetate (the substrate) is the only needed equipment. The details and results about the fabrication of the optical filters will be presented in the next section.

C. Microlens

There is available a huge number of materials for fabricating microlens. A few number of these candidate materials can be selected, e.g., SU-8/2, AZ9260 and AZ4562. These materials allow the fabrication of microlens by reflowing the raw material. This allows the production of arrays containing with a high degree of reproducibility of their characteristics.

IV. EXPERIMENTAL

A. Microlens simulation

Why using microlens in the image sensor? What is the necessity to increase the complexity of the image sensor? Figure 2 shows few FEM simulations considering impinging light from the left channel (the concept can be applied to the right channel, as well as overlapped to get the global effect) with an angle of approximately 7.6º (near the practical angles) for two cases: lenses with (a) W/L=4.8 and (b) W/L=2.4. The lenses behaviour was simulated taking into account a silicon dioxide (SiO_2) substrate. It is possible to observe the concentration of light into the direction of photodiodes (represented in the figures by pairs of black rectangles on bottom).

The simulations showed that the best results (light more concentrated) are achieved with high curvature lenses. The simulations also confirm the viability to separate the left and right channels for focusing in the respective photodiodes and for getting an estimate of the cross-talk between adjacent photodiodes (the cross-talk is smaller in the second simulation where the curvature is higher). It is assumed in the simulations that the light had already passed through the optical filters.

B. Optical filters

An array of RGB pass-band filters can be easily printed, when allowed by the printing process resolution. There are available in the market printers that allow the fabrication of optical filters with single cells of very low dimensions (with a minimum resolution of 20 µm), but their prices easily surpasses 60 k€. Despite the high cost that is initially imposed, it is expected a decrease in the cost per fabricated unit. At the current phase, the process to obtain filters were tested and characterized.

Figure 3 illustrates the selected colors for fabricating individual optical filters. After the fabrication of these optical filters by printing them into an acetate sheet, the measurements were done as follows: a monochromator was used to scan individual wavelengths along the visible spectrum and at the same time, a spectrometer measured the optical power. This procedure allowed to measurement of the optical transmittance of individual optical filters.

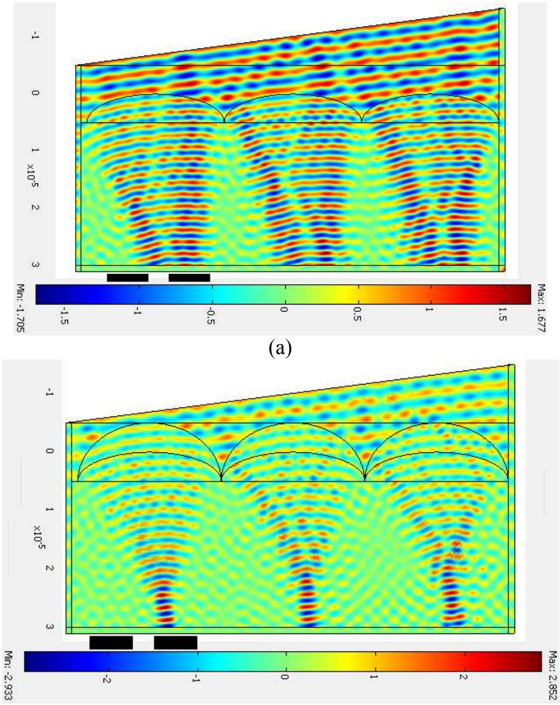

(a)

(b)

Figure 2: FEM simulations showing the light concentration into the right photodiode. The simulations where obtained respectively for lenses measuring (a) W/L=4.8 and (b) W/L=2.4. The simulations also allows to roughly estimate the degree of cross talk between two adjacent photodiodes (e.g., between the left and right channels).

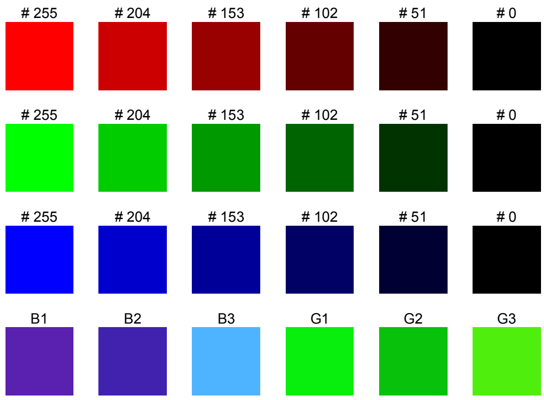

Figure 3: The used colors for fabricating the individual optical filters for further selection of the most suitable as candidate filters (those on Table I).

For the candidate filters that were selected among those with the highest potential for use in the image sensor, Table I shows their color fillings and the respective spectral measurements: the central wavelength, λ_0 [nm], and the respective full-width half-maximum, *FWHM* [nm]. Figures 4 to 6 show the amplitude spectrums of the filters listed in Table I. These spectrums were obtained by tuning the emitted wavelength with the help of a monochromator and measuring the current produced in the photodiode of the measurement instrument. As it can be observed in these Figures, the most suitable set of optical filters is the one that contains the B1, G3 and R3. This is the set that simultaneously ensures better visible band coverage and minimizes the overlap between the adjacent RGB bands.

TABLE I. FEW PRINTED RGB OPTICAL FILTERS FOR MEASURING.

Color display	Filter	RGB level [%]	λ_0 [nm]	*FWHM* [nm]
	#1 (B1)	35.3-12.5-69.0	455	120
	#2 (B2)	25.1-13.3-68.2	462	121
	#3 (B3)	30.9-70.6-100	483	101
	#1 (G1)	3.1-93.3-5.1	525	78
	#2 (G2)	2.7-75.7-4.3	525	76
	#3 (G3)	31.4-93.3-5.1	525	95
	#1 (R1)	40-0-0	NA	NA
	#2 (R2)	60-0-0	NA	NA
	#3 (R3)	100-0-0	NA	NA

Figure 6 shows only one spectrum because all filters present the same shape after doing the normalization. Figure 7 shows the pass-band spectra of the three selected filters (blue, green and red) taking into account the absolute amplitudes of the respective transmittances. This figure helps to understand why the B1, G3 and R3 filters were selected.

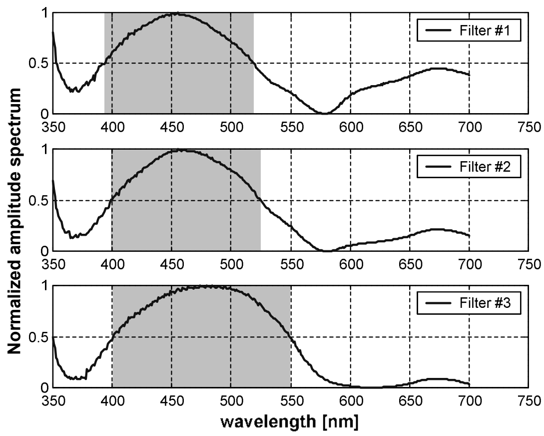

Figure 4: Amplitude spectra of blue filters listed in Table I.

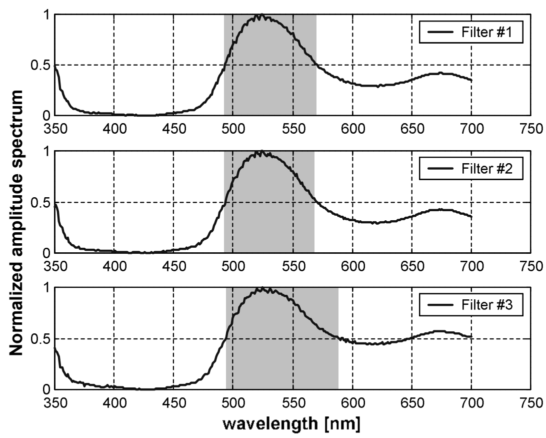

Figure 5: Amplitude spectra of green filters listed in Table I.

Few further improvements must be done with respect to the green region of the visible spectrum because even with the best optical filter (G3), it remains a slight overlap with the red region of R3 (with relative amplitude of 50%). The overlap between the blue (B1) and green (G3) is less important due to the fast decrease of both plots when within the adjacent region.

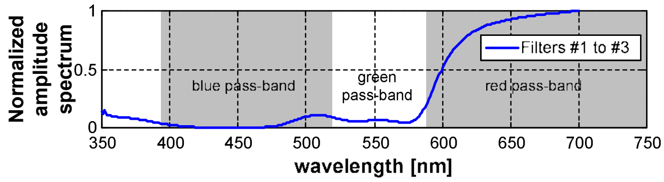

Figure 6: Amplitude spectra of red filters listed in Table I.

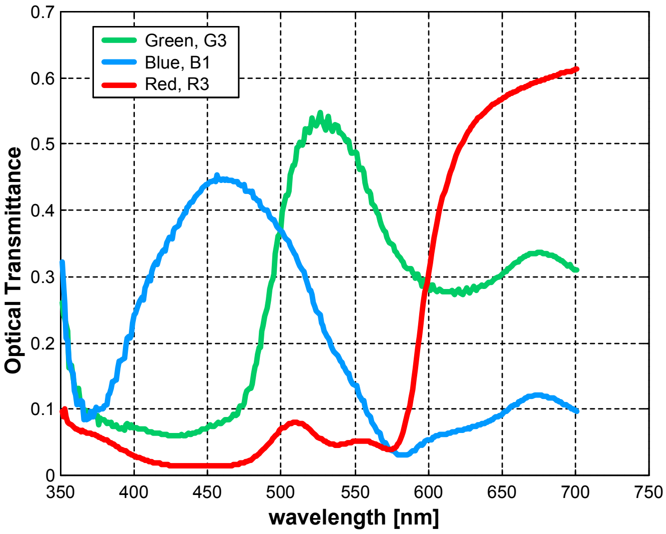

Figure 7: Amplitude spectra of the RGB filters (B1, G3 and R3) that were selected for fabricating the optical filtering prototype to use in the optical sensor.

V. CONCLUSIONS

This paper presented a stereoscopic image sensor concept with high resolution in CMOS technology. The main contribution was proposing a fabrication technology of RGB optical filters at low-cost with the help of a laser printing into a flexible and transparent substrate (e.g., acetate). The photography of the functional prototypes showed in Figure 8 confirms the possibility of getting large arrays of optical filters. For such purpose, the fabrication process must be the same based on direct color printing into acetate using an ordinary laser printer. Despite the interesting results that were obtained, further improvements must be done because the reflectivity of the impinging light is high in the border formed by the air and the surface of the filter. The next step will be the investigation of alternative substrates with better optical properties (with respect to reflectivity) and/or the investigation of coating materials for use as adaptation layer for reducing the reflectivity of the impinging light. Nonetheless, the experimental results revealed to be promising with respect to obtain suitable spectral transmittances.

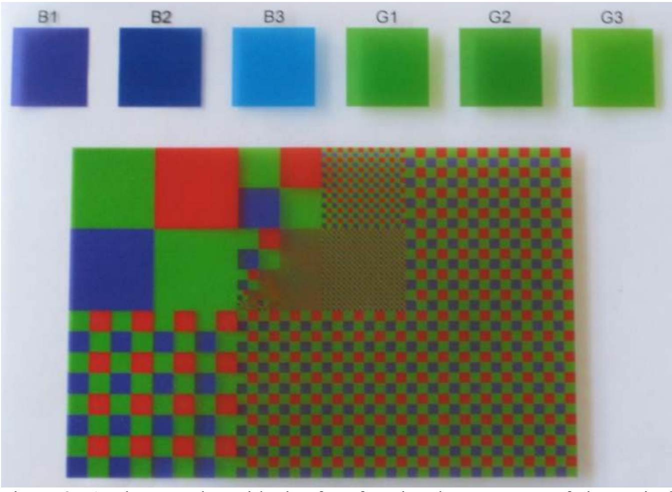

Figure 8: A photography with the few functional prototypes of the optical filters listed in Table I.

ACKNOWLEDGEMENTS

This work was fully supported by the Portuguese Foundation for Science and Technology under the project FCT/PTDC/EEA/ELC/109936/2009.

REFERENCES

[1] I. Andorko, *et al.*, "Hardware implementation of a real-time 3D video acquisition system", in proc. of 12th International Conference on Optimization of Electrical and Electronic Equipment (OPTIM 2010), Brasov, Ronaia, 20-22 May, pp. 920-925.

[2] S. Zeki, "The neurology of ambiguity", Consciousness and Cognition, Vol. 13, pp. 173-196, 2004.

[3] W. Qureshi, "Current and future applications of the capsule camera", Nature Reviews Drug Discovery, Vol. 3, pp. 447-480, May 2004.

[4] G. Iddan, *et al*, "Wireless capsule endoscopy", Nature, Vol. 405, pg. 417, May 2000.

[5] C. K. Chan, *et al*, "High-performance lithium battery anodes using silicon nanowires", Nature, Vol. 3, pp. 31-35, January 2008.

[6] M. Armand, M. Tarascon, "Building better batteries", Nature, Vol. 451, pp. 652-657, February 2008.

[7] G. Minas, *et al*, " An array of highly selective Fabry–Perot optical channels for biological fluid analysis by optical absorption using a white light source for illumination", Journal of Optics A: Pure and Applied Optics, IOP Publisher,8, pp. 272-278, 2006.

[8] G. Minas, *et al*, "An MCM-based microsystem for colorimetric detection of biomolecules in biological fluids", IEEE Sensors Journal, Vol. 6, No. 4, pp. 1003-1009, August 2006.

[9] J. Dubois, *et al*, "A 10 000 fps CMOS sensor with massively parallel image processing", IEEE Journal of Solid-State Circuits, Vol. 43, No. 3, pp. 706-717, March 2008.

[10] M. Mori, *et al*, "1/4-Inch 2-Mpixel MOS image sensor with 1.75 transistors/pixel", IEEE Journal of Solid-State Circuits, Vol. 39, No. 12, pp. 2426-2430, December 2004.